

SLAC-TN-70-5
E. Bloom, K. Doty,
G. Johnson, H. Piel,
and R. Siemann
March 1970

This is an internal informal note
not to be abstracted, quoted or
further disclosed without approval
of the author.

MULTIWIRE PROPORTIONAL CHAMBERS

This note is a summary of the work to date on the development of multiwire proportional chambers at SLAC. The design and construction of the chambers and electronics and the testing arrangement are discussed. The contents of a note¹ describing difficulties encountered during a previous test are included. Most of the results come from a run during the December cycle; the descriptions of the beam and the electronic logic apply to this run.

The body of the chamber is constructed from phenolic epoxy glass board (see Fig. 1) glued together with Dolph's epoxy. Grooves are machined in all the faces which had contact with the epoxy to prevent glue leaking into the active area of the chamber. The windows of the chamber are made of 0.006" thick Mylar spaced 0.5" from the high voltage screen. Gas enters and leaves the chamber in this space. The high voltage screen is made from a mesh of stainless steel wires (0.0014" in diameter) with a 30% open area. Future chambers will be built with thinner, more open high-voltage screens to reduce material in the beam path. The chamber wires are 30 μ -diameter gold plated molybdenum spaced 2 mm apart. The wire plane is constructed by wrapping the wire around a printed circuit card with its center machined out. Notches machined on the edge of the card position the wire. A second printed circuit card is clamped and glued into position above the first. This holds the wire in position between the two printed circuit cards. Once glued, the wires are cut and each wire is soldered to a male printed circuit card connector which is part of the card on which the wire is initially wrapped. The outside faces of the printed circuit cards are a copper plane surrounding the machined hole; this plane serves as a guard plane. The end wires of the chamber have larger diameters to taper the field gradient; wires of 0.003", 0.005" and 0.010", respectively, are the last three wires on each end of the chamber. The test chamber has a total of 74 wires; twelve of these wires have electronic instrumentation.

Each of these twelve wires has an amplifier and emitter follower to drive $50\ \Omega$ cable. The amplifier (shown in Fig. 2) uses a Motorola MC1035 differential amplifier. The sensitivity of the amplifier is controlled by adjusting the resistor labeled R_1 in Fig. 2; this resistor controls the bias of the third stage of the amplifier. Two different biases have been tested; these are shown on the transfer characteristic in Fig. 2. When biased in condition A the amplifier does not oscillate because small noise signals do not bring the amplifier into the active region. This bias places a threshold on the third stage of the amplifier; the disadvantage of this threshold is that it introduces time slewing. Bias condition B avoids this threshold, but the increased sensitivity of the amplifier can lead to oscillations caused by ground currents. Therefore, to bias the amplifiers in condition B ground currents between amplifiers must be eliminated. Bias condition B has been used successfully during the December test.

The beam for the proportional chamber tests is shown in Fig. 3; this is the π and K beam for the 82" bubble chamber. Upstream of the pulsed magnet the beam line is shared with E-41; the beam line momentum is set for a 15.5 GeV negative pion beam by the E-41 requirements. Magnets downstream of the pulsed magnet are set to optimize the counting rate at the chamber. The proportional chamber test had at least 10 pulses per second, the intensity of which could be controlled to obtain the desired counting rate. A low-pressure truly parasitic beam would probably make developmental work as described in this note easier.

The signal that a π^- has gone through the chamber is a coincidence between two $1/8'' \times 1\frac{1}{2}''$ scintillation counters, one located in front of the chamber, the other in back. The long dimension of the counters is parallel to the beam; the counter overlap is approximately 2 mm. The electronic logic for the test is shown in Fig. 4; with this arrangement it is possible to study simultaneously the performance of a single wire and the properties of the entire chamber. Note that the counter overlap concentrates most of the events on one or two wires in the chamber. The resolving time of the coincidence between the counter signal and the wires is controlled by varying the width of the counter coincidence pulse (T). The master coincidence ($T \cdot W$) pulse width is made broad to be sure that events with more than one coincident wire are scaled only once. The chamber efficiency is given by the ratio of $(T \cdot W)/T$.²

The three major problems encountered during the October test were chamber leakage current, amplifier oscillation and chamber inefficiency. The leakage current appeared to be due to carbon filaments which had grown on the chamber wires.

At the time it was not known if these filaments were due to the gas mixture (argon-isobutane) or an incident of violent arcing in the chamber. Since then reports have reached us of the growth of carbon filaments observed in methane gas at Daresbury and the observation of the carbonization of organic gases on the wires of multi-and single-wire proportional counters. We have now switched to a gas mixture of 95% argon (99.998% pure, Matheson prepurified grade); 5% CO_2 (99.99% pure, Matheson Coleman Instrument grade); this mixture has been used through the entire December test. We plan to vary the percentages of Ar and CO_2 during future tests, but do not plan a return to organic gases.

The amplifier oscillations observed in October were due to ground current problems. For stability the amplifiers had to be run in the less sensitive bias condition (condition A). Between tests a printed circuit card was designed, and extensive studies of the ground current problem enabled us to bias the amplifiers in the more sensitive configuration (condition B) without being troubled with oscillations. The resulting increased amplifier sensitivity has decreased the resolving time and has been one of the reasons for increased efficiency.

The only other cause for inefficiency which we could find in the October test was a large gas leak. A new chamber and gas system have been built and carefully checked for gas leaks. We did not have any inefficiency problems during the December test.

The efficiency of the chamber has been measured as a function of the chamber high voltage, the singles rate on one wire, the resolving time, the position of the chamber with respect to the trigger counters, and the threshold of the wire discriminators. Figure 5 shows the result of the high voltage dependence of the efficiency; the efficiency is independent of the high voltage from 4.2 to 4.6 kV. Sparking occurs if the chamber voltage is raised above 4.6 kV. The efficiency reached in the plateau region of Fig. 5 is less than 100% because the data have not been corrected for deadtime losses.

The deadtime of a single wire has been measured by varying the counting rate of the wire. The results are shown in Fig. 6; the deadtime of a single wire is 230 ± 40 ns. The efficiency of the entire chamber extrapolated to zero rate is $99.2 \pm 0.5\%$ with an 80-ns resolving time. Note the difference in the rate dependence of the efficiency of the entire chamber and of a single wire; this is an indication that the probability of a single particle counting on more than one wire is not zero. The single-wire deadtime is approximately the amount of time the primary electrons

produced near the high voltage screen take to drift to the wire; it is hoped that a narrower chamber gap will reduce the deadtime.

The dependence of the efficiency on the resolving time of the coincidence between the counters and the wires is shown in Fig. 7. The efficiency is independent of the resolving time for resolving times greater than 60 ns; this is consistent with jitter-time measurements made with a time-to-pulse height converter.

The spatial resolution of the chamber has been studied by varying the position of the chamber with respect to the trigger counters (recall that the counter overlap is only 2 mm). Figure 8a shows the results of moving the chamber in 0.5 mm steps. The efficiency of the chamber as the position is changed is shown in Fig. 8b. Although no significant deviations from uniform efficiency are seen, there are slight dips when the particle beam is between wires. More accurate data are needed to know if these dips are real.

The spatial resolution data can be used to give an approximate measure of the number of wires that count per particle traversing the chamber. The result is that 1.15 wires count per particle; a thinner chamber should improve this number.

Figure 9 shows the dependence of the efficiency of a single wire on the threshold of the discriminator of that wire. When examined with an oscilloscope (see Fig. 10) the amplifier output pulses are 500 to 600 mV in amplitude (consistent with the discriminator curve) and 200-300 ns long (consistent with the measured deadtime).

The next chamber we will be building will have a 4 mm gap between high voltage screen and wires and will use $20\ \mu$ -diameter wires. This chamber will be put in the 20 GeV spectrometer to test the reliability of the chamber over a long period of time. In addition, low cost instrumentation for each wire is being designed, and studies are planned to find ways to reduce the resolving time.

We have built and tested multiwire proportional chambers at SLAC. We are able to report time resolutions of 60 ns FWHM and spatial resolutions of approximately 2 mm.

Footnotes

1. Memo of October 27, 1969 from E. Bloom, K. Doty, G. Johnson, and R. Siemann.
2. To precisely determine the efficiency, corrections must be made for accidental triggers and accidental coincidences between the trigger and wires. This correction depends on experimental arrangement. The corrected number of triggers is

$$T_c = T - T_\delta (1 - P_f)(1 - P_b)$$

where

T \equiv number of coincidences between counters,

T_δ \equiv number of accidental coincidences between counters,

$P_{f(b)}$ \equiv probability that a particle going through the front (back) counter will count on one of the active wires.

Typically, $T_\delta/T \lesssim 3\%$, $P_f \sim 95\%$, $P_b \sim 96\%$. The total correction is less than 0.01%. The corrected number of coincidences between wires is

$$T \cdot W_c = T \cdot W - T \cdot W_\delta (1 - \epsilon),$$

where

$T \cdot W$ \equiv number of coincidences between counters and wires,

$T \cdot W_\delta$ \equiv number of accidental coincidences between counters and wires,

ϵ \equiv efficiency of the chamber.

Solving for the efficiency, one gets

$$\epsilon = (T \cdot W_c) / T_c = \frac{T \cdot W - T \cdot W_\delta (1 - \epsilon)}{T_c}$$

or

$$\epsilon = \frac{T \cdot W - T \cdot W_\delta}{T_c - T \cdot W_\delta} .$$

This is the exact expression used in calculating the efficiency.

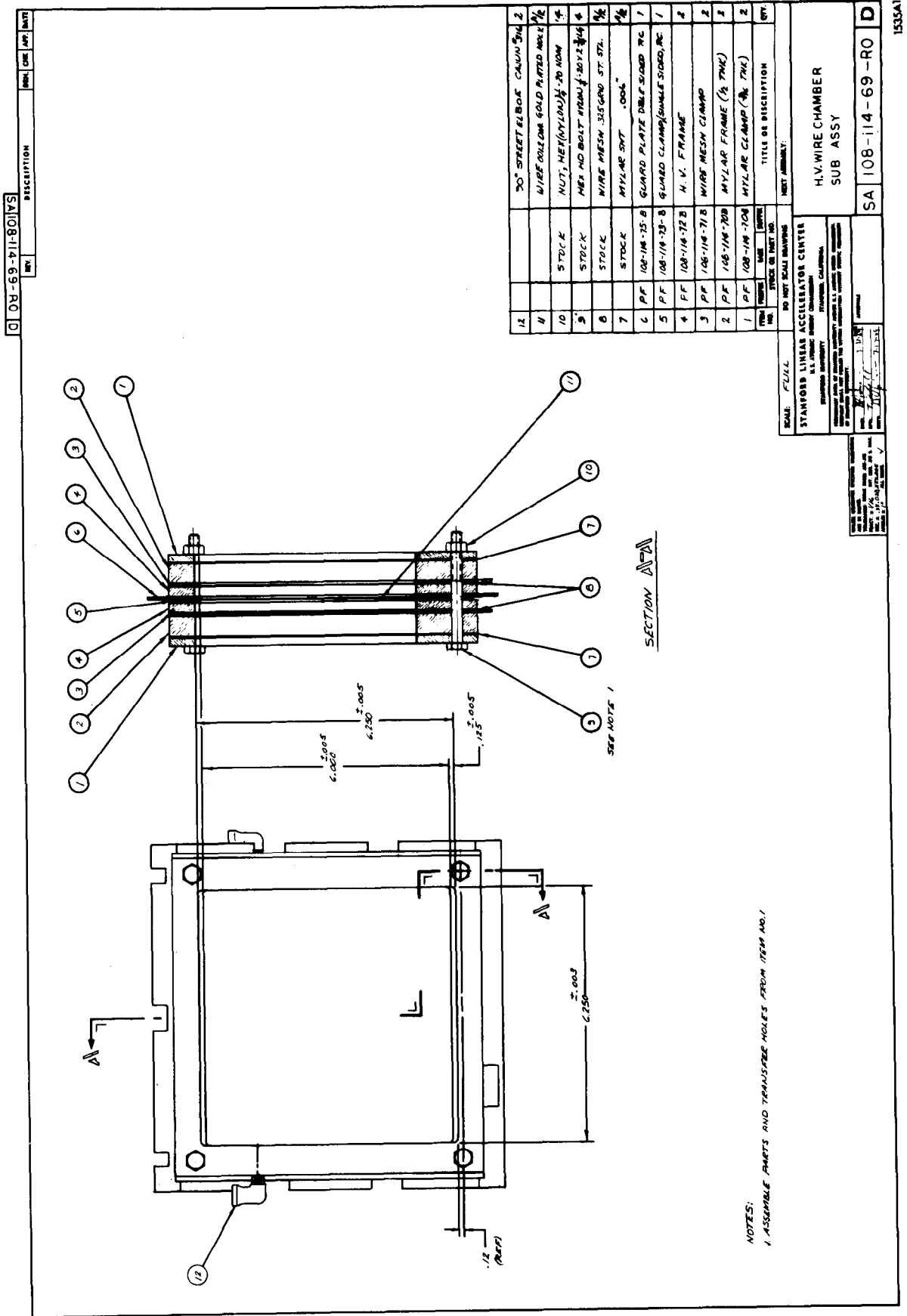


FIG. 1

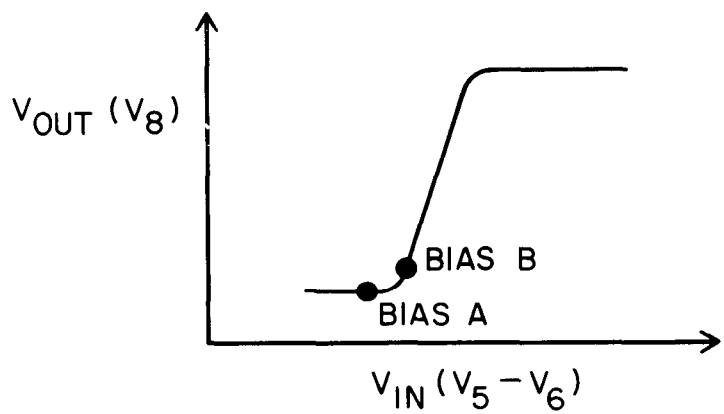
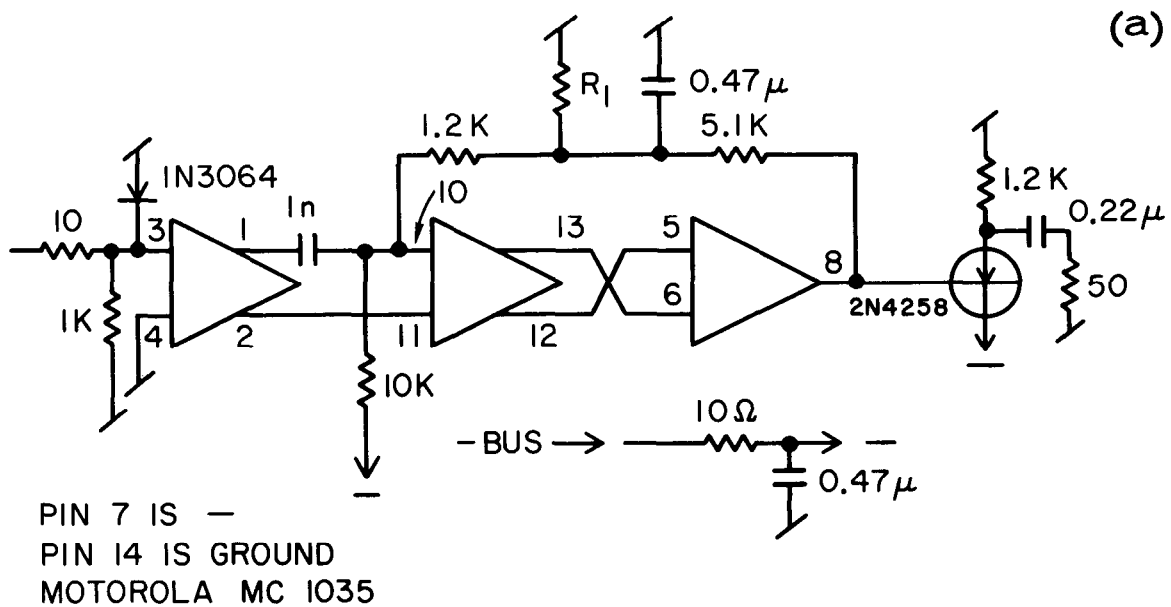


FIG. 2-- a) Proportional chamber amplifier.
 b) Single stage amplifier transfer characteristic.

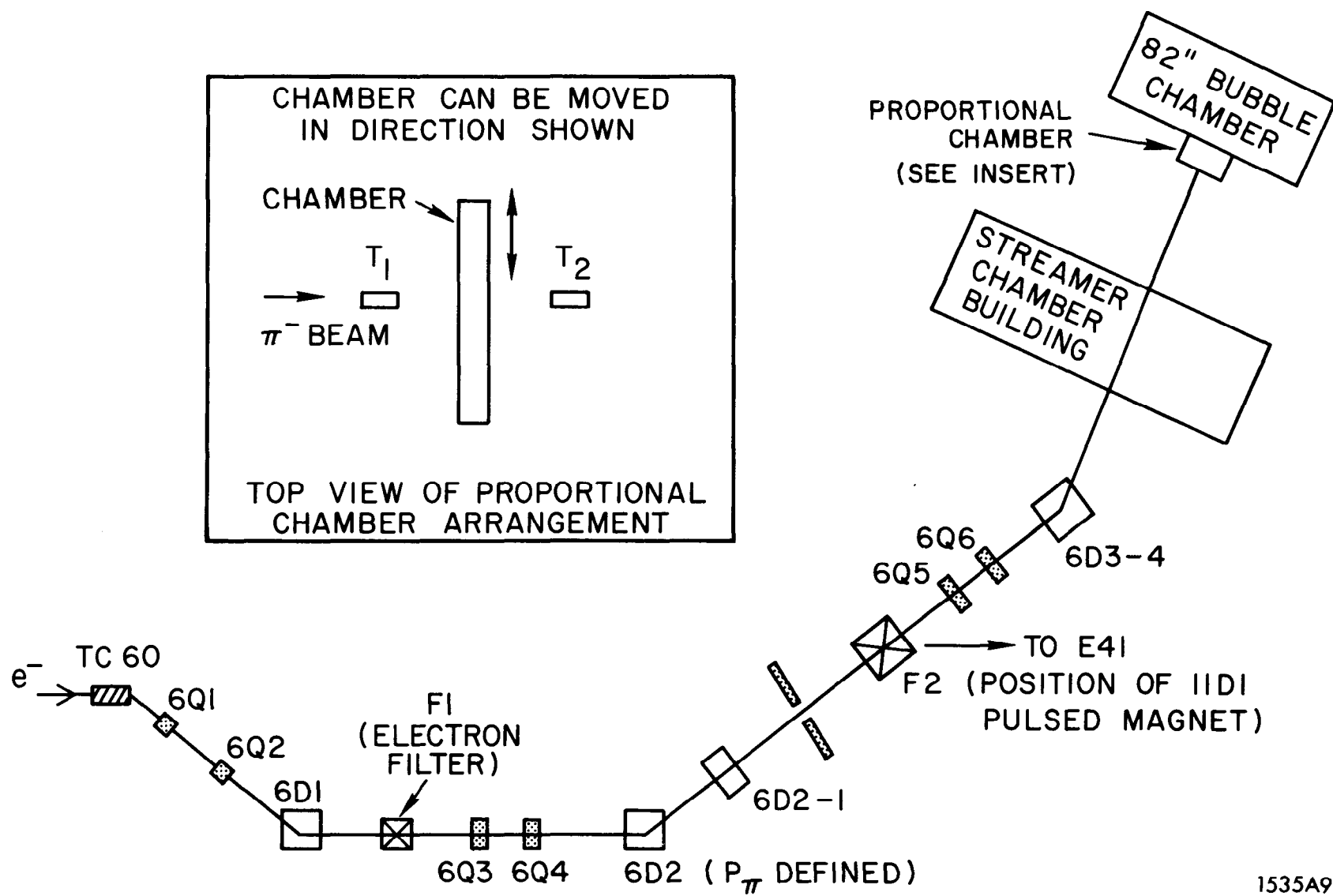


FIG. 3--Experimental beam line and setup.

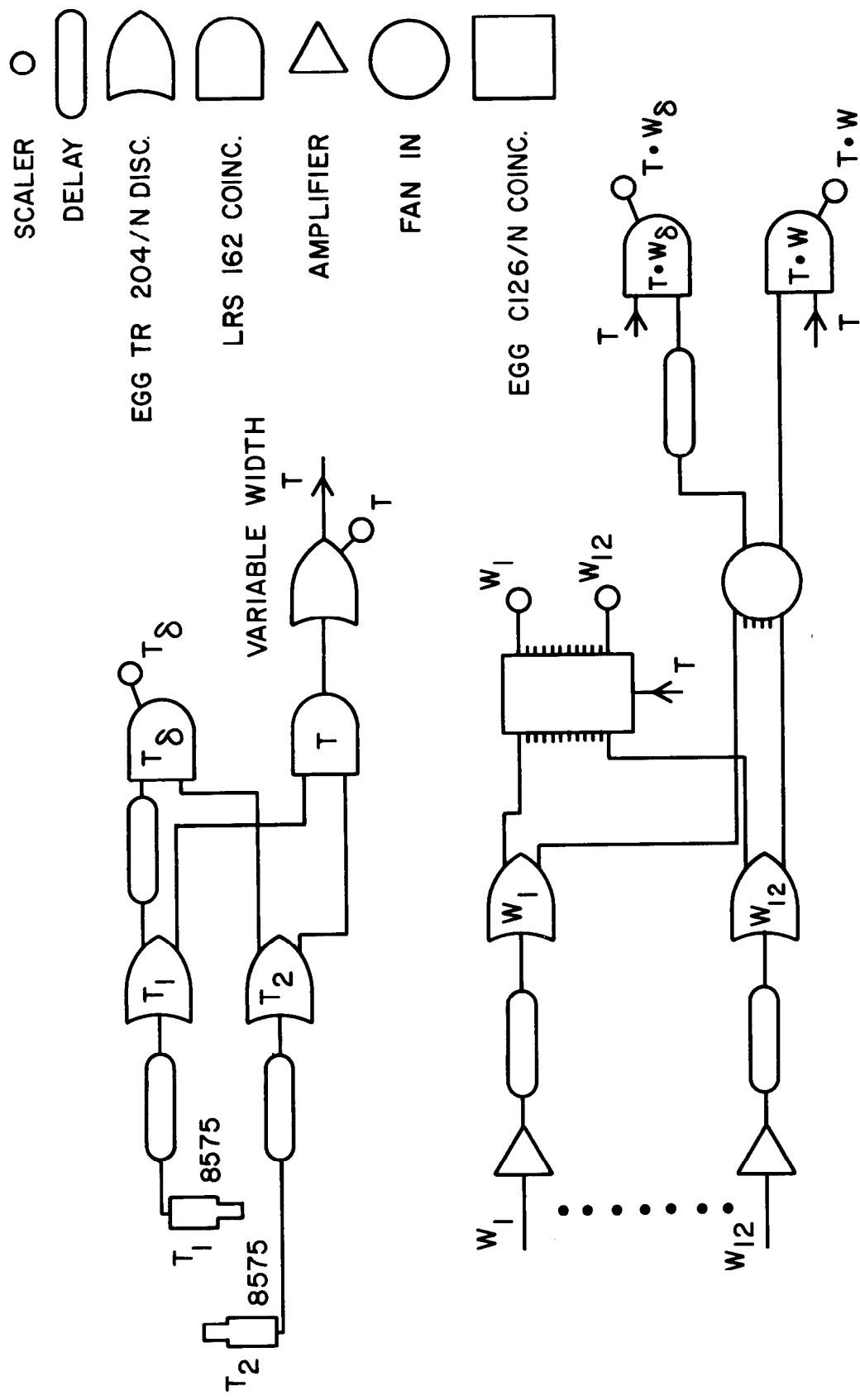


FIG. 4--Trigger definition and wire logic diagrams.

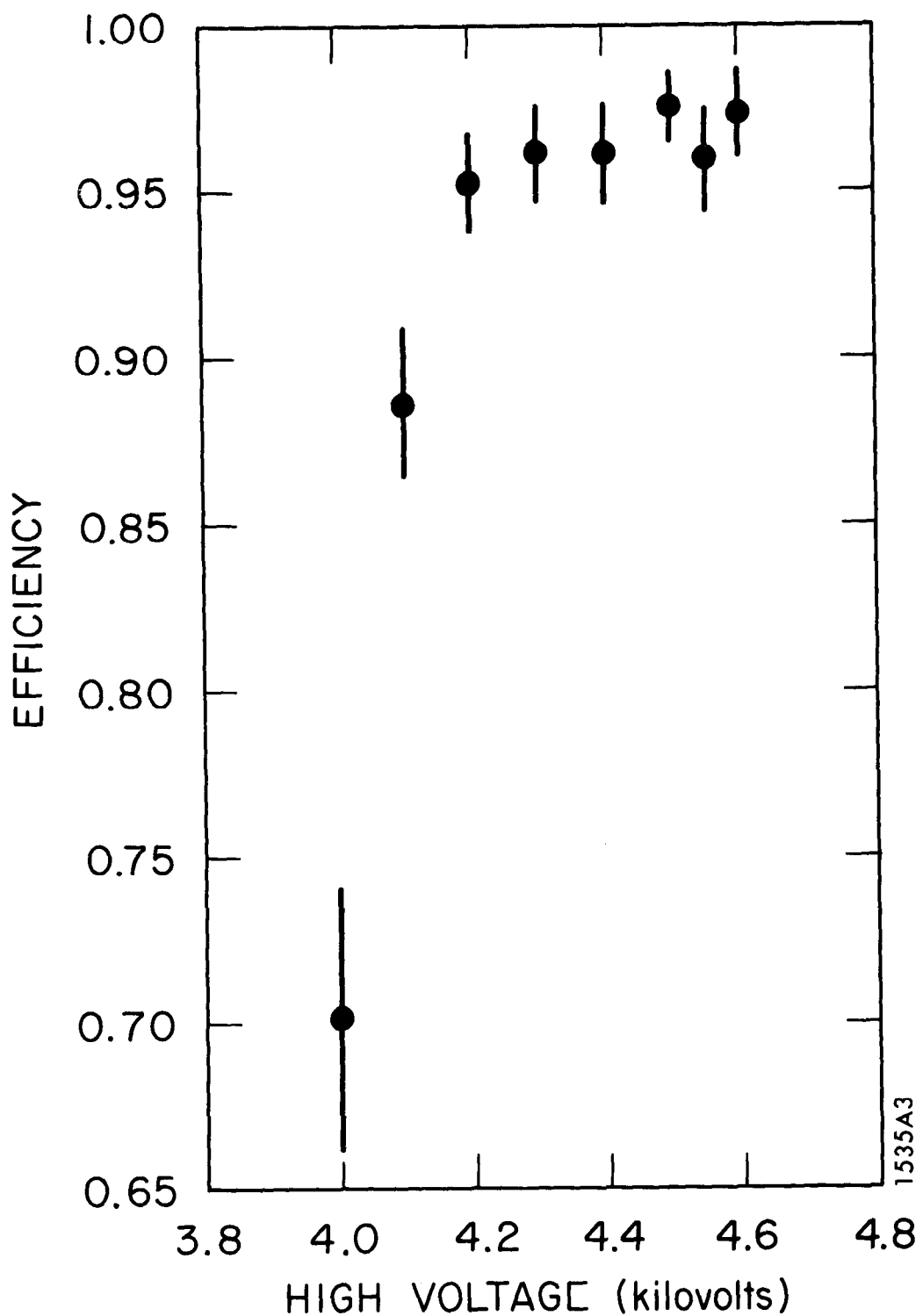


FIG. 5--Efficiency versus chamber high voltage.

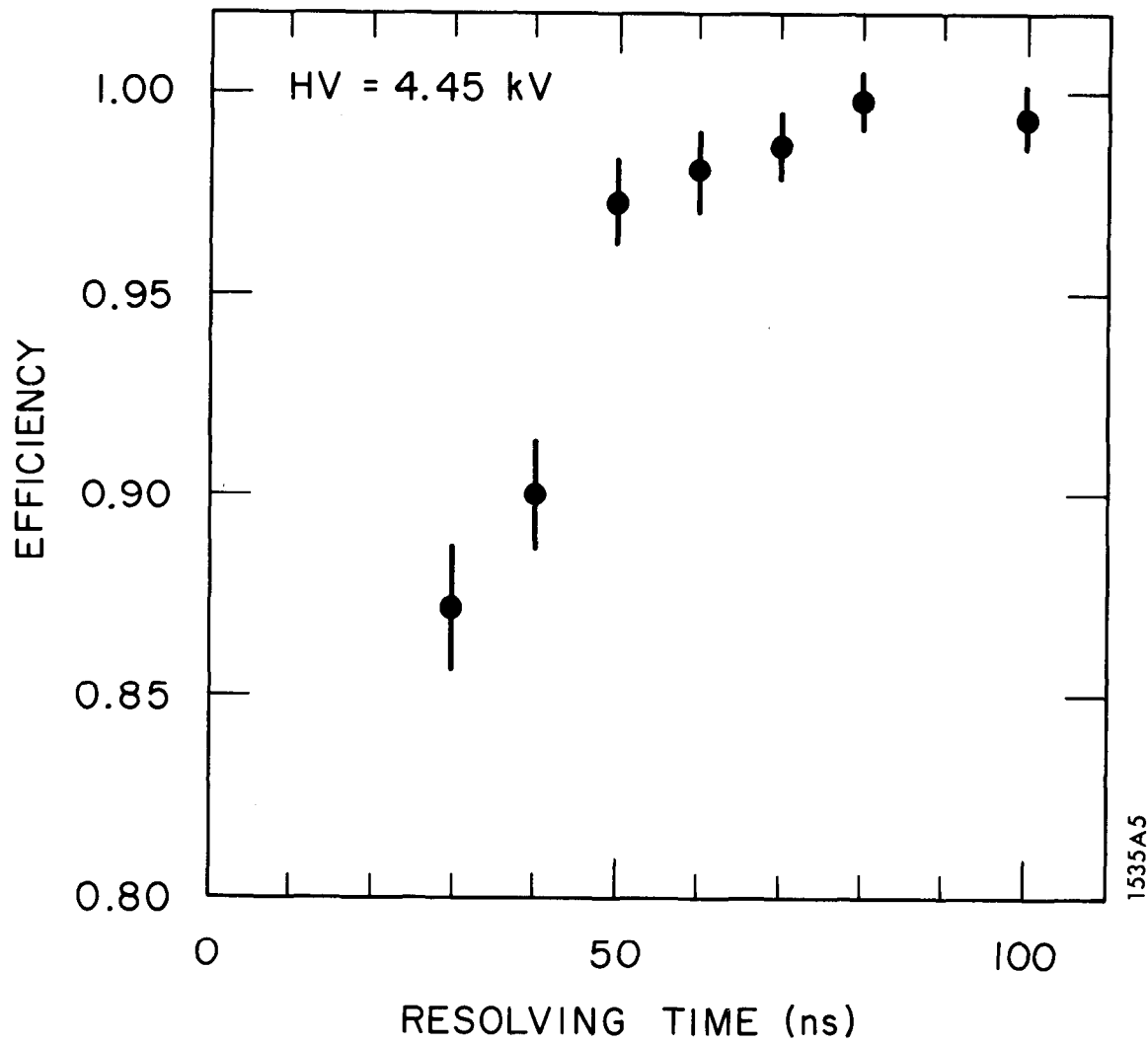


FIG. 7--Efficiency versus resolving time. Dead time corrections (less than 2%) have been made.

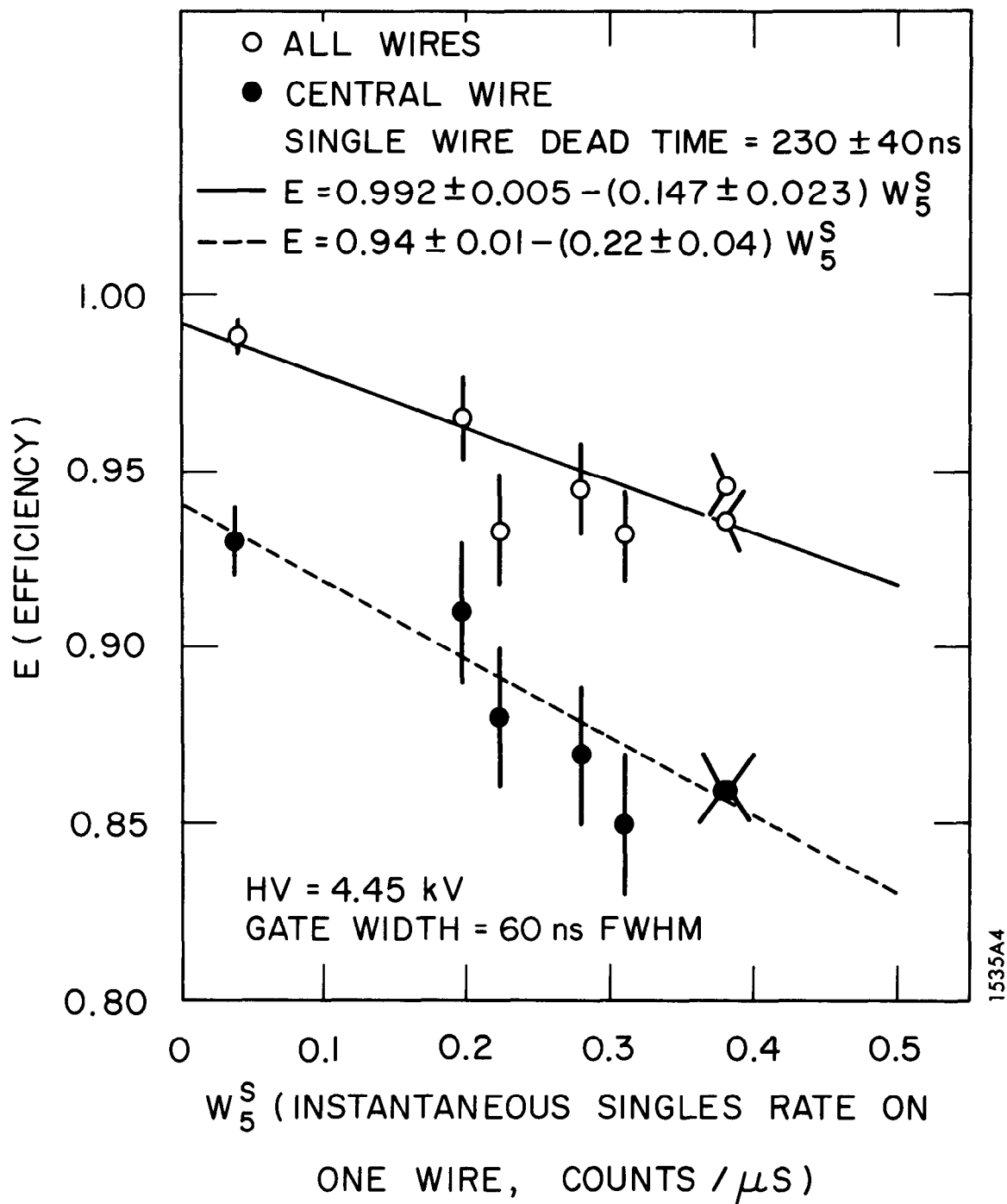


FIG. 6--Efficiency versus instantaneous singles rate on one wire.

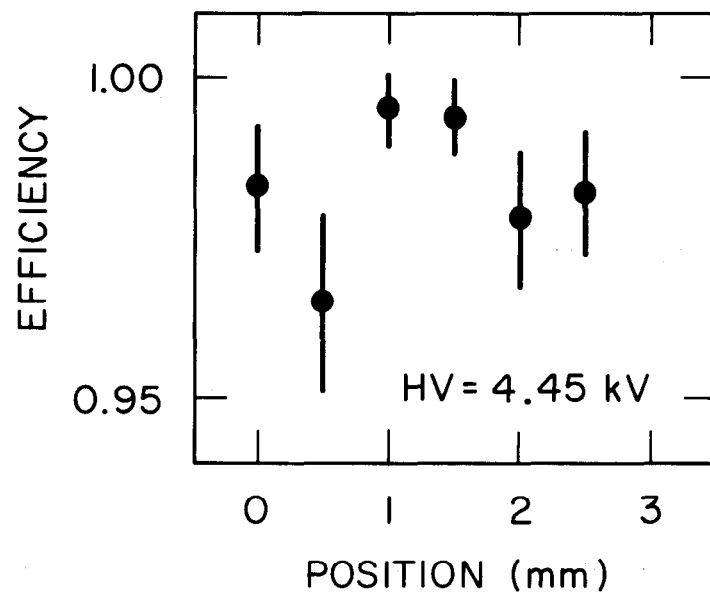
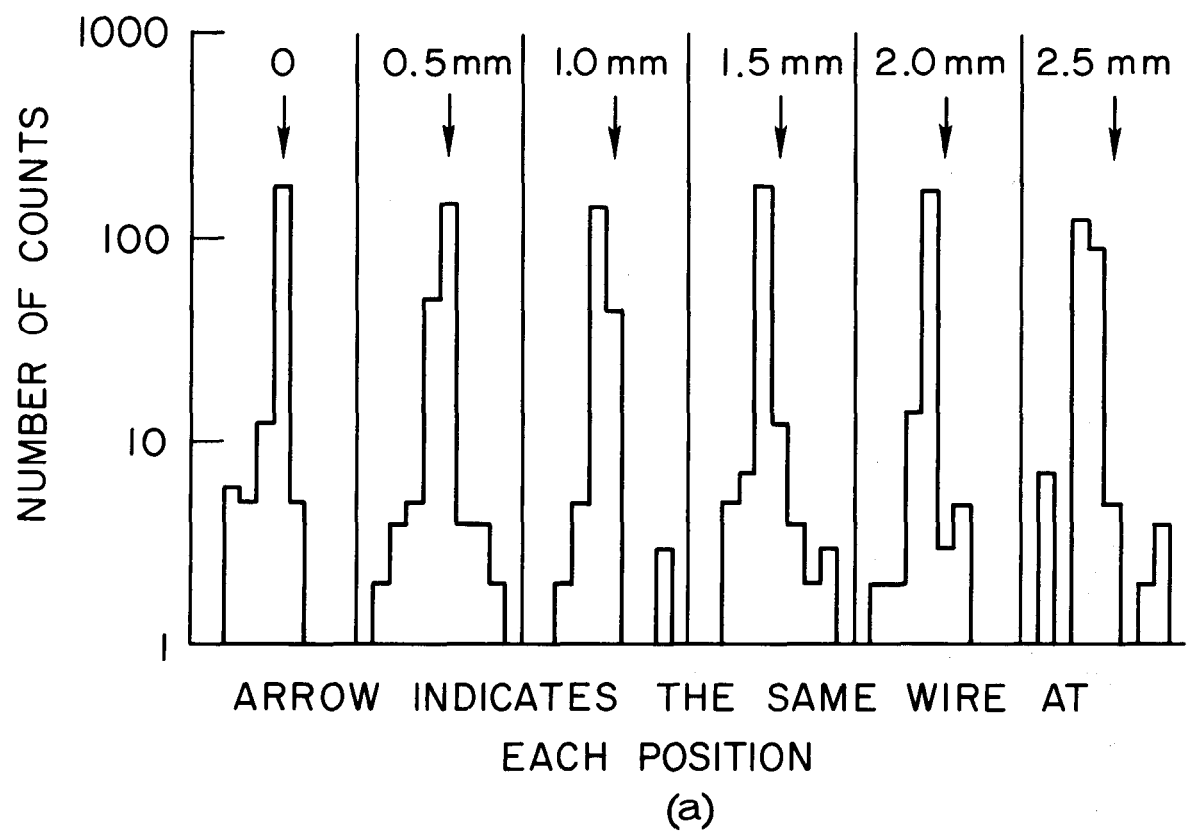


FIG. 8-- a) Number of counts versus chamber position.
 b) Efficiency versus position of chamber.

1535A6

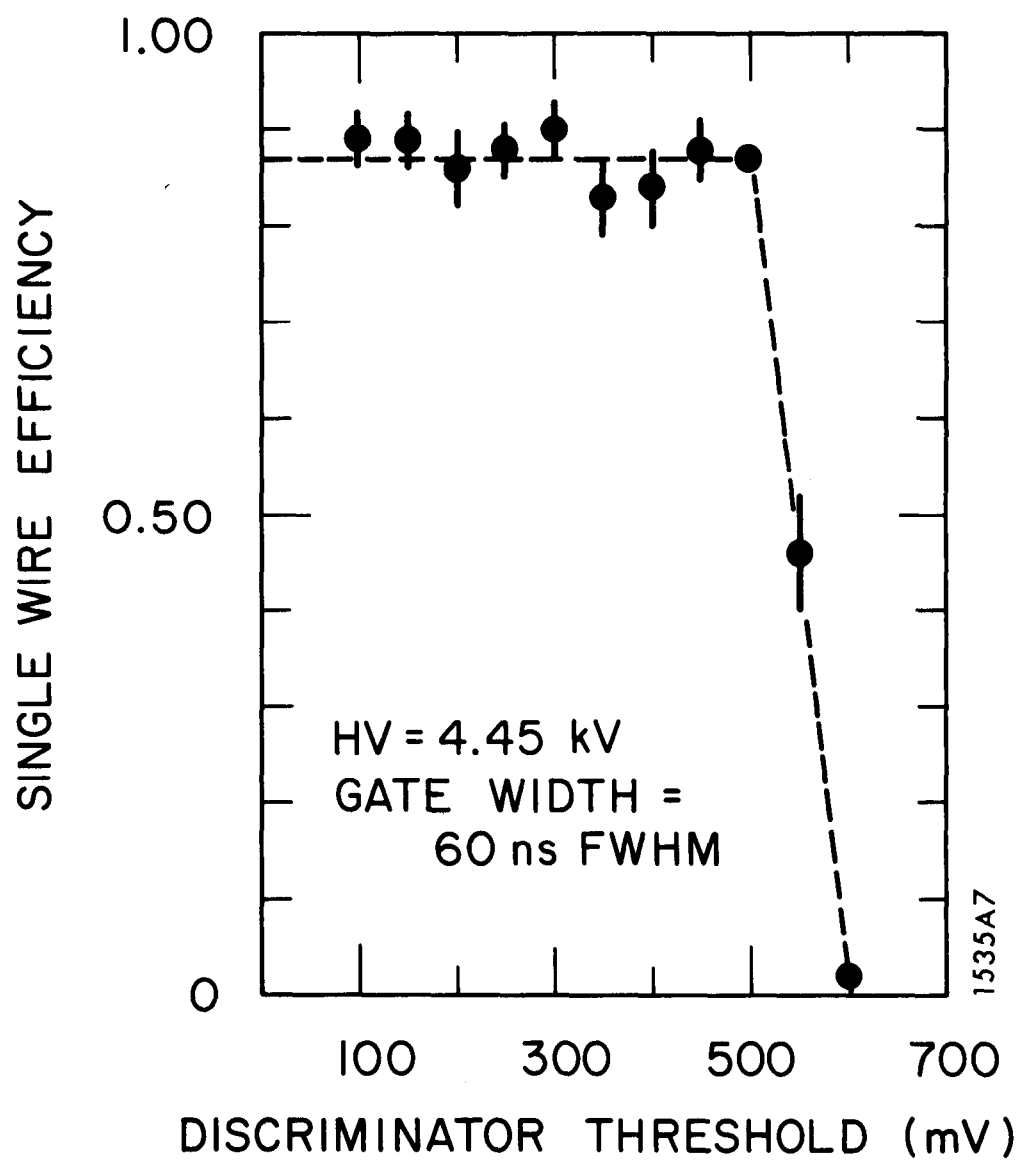
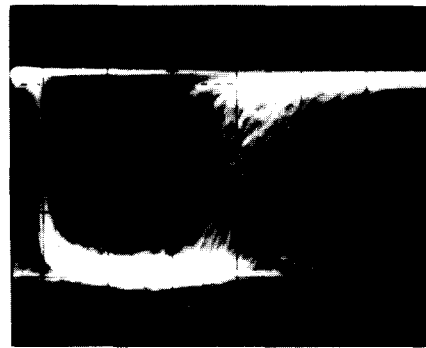


FIG. 9--Single wire efficiency versus discriminator threshold.



1535A8

FIG. 10--Amplifier output pulses.

Sweep speed: 100 nsec/cm.
Amplitude: 200 mV/cm.

